Proglacial methane emissions driven by meltwater and groundwater flushing in a high Arctic glacial catchment

Gabrielle E. Kleber[1,2,3], Leonard Magerl[3], Alexandra V. Turchyn[3], Mark Trimmer[4], Yizhu Zhu[4], Andrew Hodson[2,5]

[1]Department of Earth Sciences, University of Cambridge, Cambridge CB2 3EQ, UK
[2]Arctic Geology, University Centre in Svalbard (UNIS), Longyearbyen, 9170 Norway
[3]Department of Geoscience, UiT the Arctic University of Norway, Tromsø, 9010 Norway
[4]School of Biological and Behavioural Sciences, Queen Mary University of London E1 4NS, London, UK
[5]Department of Environmental Sciences, Western Norway University of Applied Sciences, Sogndal, 6856 Norway

Correspondence to: Gabrielle E. Kleber (gakle2914@uit.no)

Abstract. Glacial groundwater releases geologic methane in areas of glacier retreat on Svalbard, representing a large, climate-sensitive source of the greenhouse gas. Methane emissions from glacial melt rivers are known to occur in other regions of the Arctic, but such emissions have not yet been considered on Svalbard. Over two summers, we monitored methane concentrations in the proglacial groundwater springs and river network of a 20 km2 valley glacier in central Svalbard to estimate melt season emissions from a single catchment. We found that methane concentrations in the glacial river reach up to 3170 nM, which is nearly 800-times higher than the atmospheric equilibrial concentration. We estimate a total of 1.0 ton of melt season methane emissions from the catchment, of which nearly two-thirds are being flushed from the glacier bed by the melt river. These findings provide further evidence that terrestrial glacier forefields on Svalbard are hotspots for methane emissions, with a climate feedback loop driven by glacier melt. As the first investigation into methane emissions from glacial melt rivers on Svalbard, our study suggests that summer meltwater flushing of methane from the ~1400 land-terminating glaciers across Svalbard may represent an important seasonal source of emissions. Furthermore, glacial melt rivers may be a growing emission source across other rapidly warming regions of the Arctic.

1 Introduction

The Arctic region plays an important role for global methane emissions, largely from natural sources such as wetlands, permafrost and geological seeps. In recent decades, seasonal and climatic controls on methane emissions from these climate-sensitive systems have been observed (McGuire et al., 2009; Schuur et al., 2015; Walter Anthony et al., 2012; Yvon-Durocher et al., 2014; Zona et al., 2016), highlighting their vulnerability to rising temperatures and changes in seasonal patterns. This has led researchers to predict further increases in natural methane emissions from across the Arctic as global temperatures continue to rise—a positive feedback that contributes to the amplification of warming in the Arctic and may increase the rate of future climate change (Schuur et al., 2008). Decades of observational records support this 'Arctic amplification' and suggest that the Arctic is warming at a rate up to four-times faster than the global average (Rantanen et al., 2022).

The Arctic hosts a large reservoir of organic carbon (Gautier et al., 2009; Hugelius et al., 2014; Isaksen et al., 2011) which is stored in permafrost, natural gas deposits and coal beds. With sufficiently low temperatures and high pressures, volatile

35   compounds like ethane and methane can be stored in a solid state in the form of gas hydrates. This carbon can be released to the atmosphere as methane gas primarily by the microbial degradation of organic carbon once it becomes bioavailable via permafrost thaw or, alternatively, by the dissociation of gas hydrates and direct release in response to climate warming. A growing body of research has identified additional pathways for natural methane emissions at the boundaries of glacial retreat in the Arctic, where active releases of both microbially-produced and geologic methane have been found to exist (Christiansen

40   and Jørgensen, 2018; Kleber et al., 2023; Lamarche-Gagnon et al., 2019; Walter Anthony et al., 2012).

The advance of glaciers over vegetation secures a subglacial reservoir of organic carbon that can be microbially degraded into methane, which is then trapped by the overburden of the overlying glacier and accumulates. Studies have detected methane releases at margins of retreating ice sheets and glaciers in Canada, Greenland and Iceland, where microbially-produced

45   methane in the anoxic environment of the glacier bed is transported by meltwater and degassed to the atmosphere (Burns et al., 2018; Christiansen et al., 2021; Christiansen and Jørgensen, 2018; Dieser et al., 2014; Lamarche-Gagnon et al., 2019; Pain et al., 2020; Sapper et al., 2023). The findings of Lamarche-Gagnon et al (2019) suggest that the methane reserves beneath the Greenland Ice Sheet greatly exceed the methane transported to its margin, and thus increased melt in the future may lead to increased export and release of methane.

50

Alternatively, studies in Alaska and Arctic Norway have identified climate-sensitive releases of ancient geologic methane. In regions of permafrost thaw and glacier retreat, methane that was previously stored within rocks and trapped beneath a 'cryospheric cap' of glaciers and permafrost is now migrating to the surface and being released to the atmosphere (Kleber et al., 2023; Walter Anthony et al., 2012). Over 100 of these seeps have been identified across a region of Svalbard in the

55   Norwegian High Arctic, where methane is brought to the surface by groundwater springs that form in the exposed forefields of retreating glaciers (Kleber et al., 2023). Emissions from these sources are expected to increase as more land is exposed by accelerating glacier melt.

The seasonality, extent, and the governing mechanisms of climate-enhanced methane emissions in the Arctic are still largely

60   unknown and thus difficult to quantify. As such, these emission sources represent a large uncertainty for the Arctic methane budget and are yet to be included. Our study focuses on one glacial catchment on Svalbard, where we monitor methane sources in the glacial forefield, including the glacial melt river and groundwater springs, and estimate their potential seasonal emissions to the atmosphere.

2 Methods

2.1 Site description and field study

65

Our study is based in the catchment of the Vallåkrabreen glacier, a ~20 km^2 valley glacier located in central Svalbard (Fig. 1a). Vallåkrabreen is situated most prominently within the Carolinefjellet geological formation, a lithostratigraphic unit comprised of Lower Cretaceous organic-rich successions of fine-grained shales and sandstones. The Carolinefjellet Formation is a known petroleum source rock with inclusions of oil-associated thermogenic C_1-C_4 gases (Abay et al., 2017). The field

70 study took place between July-September of 2021 and 2022. We measure methane concentrations in the glacial melt river and groundwater streams to estimate potential melt season methane emissions due to degassing. In addition, we measure methane ebullition (bubbling of gas) from vents within groundwater pools.
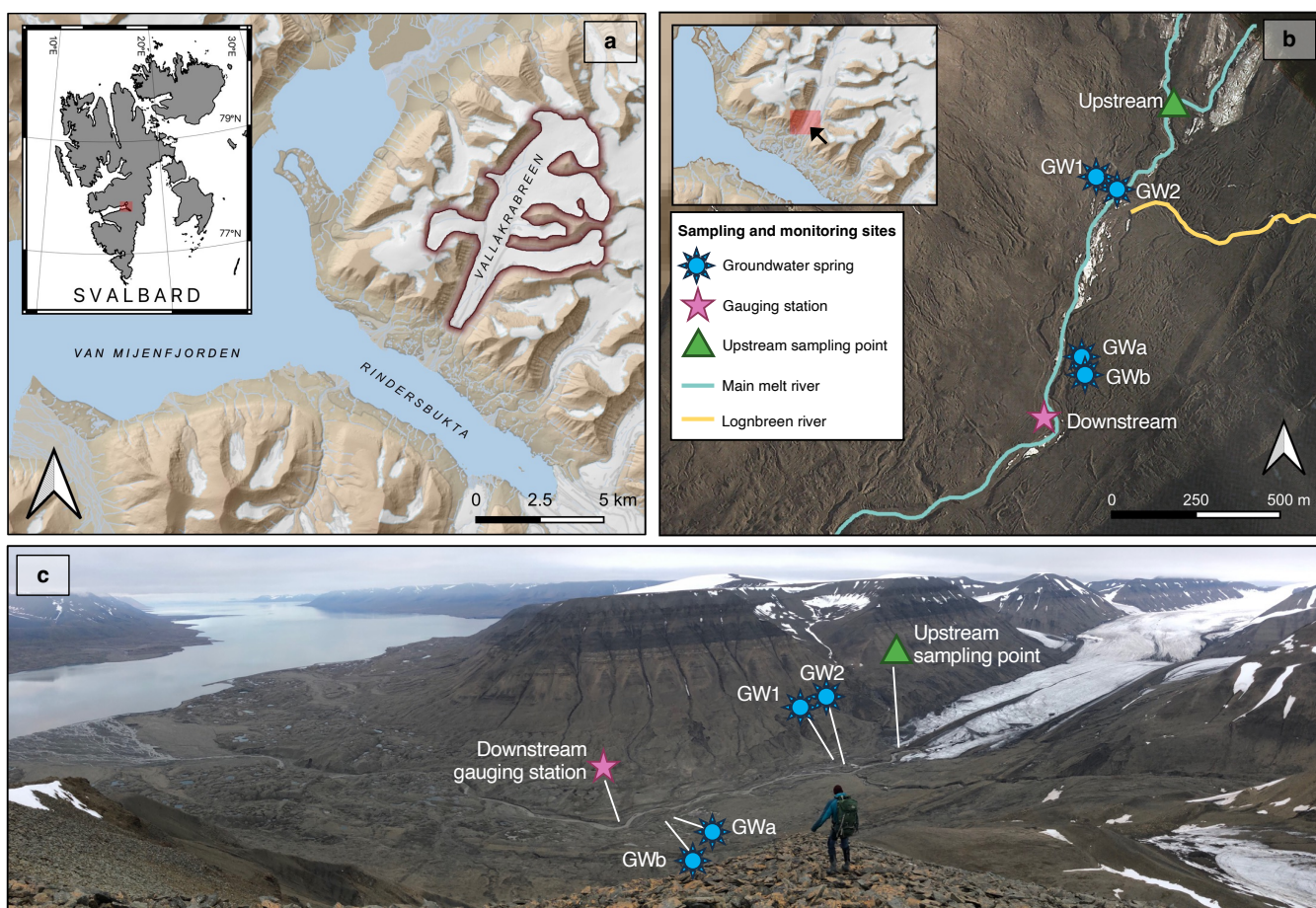
75 **Figure 1. Overview of the Vallåkrabreen catchment. (a) Location of Vallåkrabreen on the Svalbard archipelago (base map data provided by the Norwegian Polar Institute), (b) location of sampling sites and the gauging station (satellite image retrieved on 07**

July 2022 by Kompsat-2), (c) photo of the Vallåkrabreen catchment, taken from the location marked by the black arrow on the inset map in panel b.

80   Water samples were taken to measure methane concentrations in the glacial melt river every 2-5 days during the summer of 2021 at an 'upstream' site approximately 100 m downstream of the confluence of the glacier's two rivers: (1) a river flowing from a subglacial portal and (2) a stream flowing from a supraglacial channel. Samples were also taken at the same frequency at a gauging station that was installed in the melt river approximately 1000 m downstream from the upstream sampling point. Hourly discharge measurements of the bulk melt river were derived from measurements taken at the gauging station. Samples

85   of two groundwater springs (GW1 and GW2) within the glacier forefield were taken every 2-5 days during the summers of 2021 and 2022 and their methane concentrations, along with the isotopic composition of the methane, were published previously in Kleber et al. (2024). Groundwater outflow rates were measured periodically from the two main groundwater springs. In addition, repeated measurements of methane ebullition were taken from vents within groundwater pools, and one-time chamber measurements were taken of the diffusive flux of methane from sediments within the glacier forefield. A detailed

90   map of the field site is provided in Fig. 1 and includes the upstream melt river sampling point and gauging station, and the location of the groundwater springs.

2.2 Sampling and laboratory analysis

2.2.1 Measurement of aqueous methane in river and groundwater

    Samples were taken for the measurement of aqueous methane concentrations by submerging 20 mL glass vials directly into

95   the turbulent, well-mixed stream and capping with a gas-tight crimped cap. To prevent microbial activity during storage, samples were fixed within 24 hours with 1 mL of 1 M NaOH, then stored upside-down in the dark at approximately 4°C until analysis. The measurement of water methane concentration was conducted using the headspace method as described in Kleber et al. (2023), on a gas chromatograph fitted with a flame ionization detector (GC-FID, Agilent Technologies UK Ltd., South Queensferry, UK) at the Queen Mary University of London. Methane concentration measurements were within an analytical

100   error of 5.5%, calculated as two-times the standard deviation of repeat measurements of 100 ppm standards ($n = 12$), and a lower detection limit of 18 nM. The stable carbon isotopic composition of methane ($\delta^{13}C$-CH_4) was analysed in samples with sufficiently high methane concentrations at the University of Cambridge in the LASER-ENVI facility using a cavity ringdown spectrometer (Picarro G2201-I, Picarro Inc., Santa Clara, California, U.S.A.). Values are reported relative to the Vienna Pee Dee Belemnite (VPDB) standard and an analytical error of 0.1‰.

2.2.2 Groundwater outflow measurements

Discharge measurements of the groundwater outflows were made using the float method (Turnipseed and Sauer, 2010) periodically throughout the summer and are within an error of 18% based on the standard deviation of repeat measurements ($n = 10$).

2.2.3 Hydrological monitoring of the melt river

Total discharge from the main melt river was calculated using hourly stage measurements made by a Druck CS420 pressure transducer at the downstream gauging station from 03 July to 15 September 2021. The rate of discharge was measured periodically using a fluorescent Rhodamine WT dye tracing method and fluorometer, as described by Wilson et al. (1986). Hourly stage measurements were converted to hourly discharge rates using a calibration curve (Supplementary Fig. S.1) calculated with 8 discrete discharge measurements. The calculated melt river discharge had an error of 17%, based on the greatest difference between 8 discharge measurements through dye tracing and the corresponding discharge calculated by the calibration curve.

2.2.4 Ebullition measurements

Measurements of methane emissions via ebullition were made using a bespoke bubble trap as described in Walter et al. (2006), which funnelled all gas bubbles released from an individual vent into a plastic bottle of known volume (Supplementary Fig. S.2). Repeat measurements were made periodically on five discrete vents throughout the summer. Five mL of the collected gas were extracted from the bottle and injected into a pre-evacuated 3 mL Exetainer vial. Methane concentrations of ebullition samples were analysed at the University of Cambridge in the LASER-ENVI facility using a cavity ringdown spectrometer (Picarro G2201-I, Picarro Inc., Santa Clara, California, U.S.A.).

2.3 Potential emission calculations

We calculate potential methane emissions from groundwater outflows and the melt river, which represent the amount of methane transported to the proglacial area by these systems. Potential emissions are calculated using a mass balance approach (Hodson et al., 2019), described in its basic form in Equation 1. For a single glacial input that equilibrates with the atmosphere before discharge into the sea, the mass balance-defined emission flux, F_{atm}, is

$$F_{atm} = (C_{in} - C_a) \times Q_{in} ,$$ (1)

where Q_{in} is the discharge input to the proglacial area with methane concentration C_{in} less the atmospheric equilibrium concentration (C_a, ~4 nM for fresh water at 0°C with an atmosphere of 1.8 ppm methane). The potential emissions assume that all methane above the atmospheric equilibrium concentration is degassed to the atmosphere. The likelihood of any

consumption of the methane by microbial oxidation before it can be released to the atmosphere is addressed in the discussion section.

2.3.1 Potential melt season methane emissions from groundwater

The equation used to calculate potential methane emissions from groundwater spring x, F_x (kg hr^{-1}), is as follows:

$$F_x = (C_{x,CH_4} - 4) \times a \times Q_x \times 10^{-6}, \tag{2}$$

where C_{x,CH_4} is the average concentration of methane (nM) in the outflow of groundwater spring x, cited from Kleber et al. (2024). Conversion factor, a, is used to convert methane concentration from nM to mg L^{-1} (1.6 x 10^{-5}), and Q_x is the average hourly discharge rate of the outflow (L hr^{-1}). F_x, calculated in kg hr^{-1}, is obtained by converting the methane concentration to kg L^{-1}, which is done by multiplying the whole equation by 10^{-6}. Hourly fluxes were extrapolated across the five melt season months.

2.3.2 Potential melt season methane emissions from the melt river

Potential melt season methane emissions from the melt river, F_{riv} (kg a^{-1}) are calculated on an hourly basis and summed using the following equation:

$$F_{riv} = \sum_{i=1}^{n}(C_{i,CH_4} - 4) \times a \times Q_i \times 10^3 \times 3600 \times 10^6, \tag{3}$$

where C_{i,CH_4} is the hourly concentration of the upstream river at the upstream sampling point (nM) determined by linear interpolation between measured samples, a is a conversion factor to convert methane concentration from nM to mg L^{-1} (1.6 x 10^{-5}), and Q_i is the discharge rate of the river measured hourly (m^3 s^{-1}) which is converted to hourly discharge in L hr^{-1} by multiplying by 10^3 and multiplying by 3600. The discharge rate is derived by stage measurements at hour i, and n represents the number of hours in the summer. F_{riv}, calculated in kg summer^{-1}, is obtained by converting the methane concentration to kg L^{-1}, which is done by multiplying the whole equation by 10^6.

The Lognbreen river (highlighted in yellow in Fig. 1b), which is fed from a small valley glacier to the east of Vallåkrabreen, enters the Vallåkrabreen river upstream of the gauging station. Therefore, the contribution of the Lognbreen river was removed from the total discharge measurements for methane emission calculations. Periodic discharge measurements of the Lognbreen river were made by salt dilutions (Turnipseed and Sauer, 2010) and compared to the total Vallåkrabreen discharge rate at the corresponding time. The percent contribution from the Lognbreen river averaged 10% ($n = 4$) and thus the discharge rates of the Vallåkrabreen river were reduced by 10% for the calculation of methane emissions. The gauging station was also downstream from the confluence of the groundwater springs measured in this study, however, their overall discharge rate consistently equated to <0.01% of the total discharge rate of the Vallåkrabreen river and thus their contribution was considered negligible.

Discharge rates of the river outside of the gauging period (26 May-02 July and 16 September-06 October) were estimated daily

165 using the relationship between mean daily air temperature measured at a weather station 10 km from Vallåkrabreen (Sveagruva, seklima.met.no) and the sum of hourly discharge per day determined throughout the sampling period (Supplementary Fig. S.3). Methane concentrations in the river at the start of the melt season and before the sampling period started (26 May-08 July) were estimated as the concentration of the first sample taken on 08 July (3172 nM). The concentrations in the river at the end of the melt season and after the sampling period ended (24 September-06 October) were estimated as the average

170 concentration of the last two samples taken at the upstream sampling point on 15 and 24 September (481 nM).

3 Results

3.1 Potential methane emissions from the melt river

Methane concentrations in the main melt river were measured at the upstream sampling point as well as at the downstream gauging station. The upstream melt river starts with high concentrations (up to 3170 nM) towards the beginning of the melt

175 season and decline to average values of about 500 nM by the end of July. The downstream samples also begin the season with high concentrations (1000 nM) and decline to an average of ~440 nM for the remainder of the summer. Seasonal methane concentrations of the upstream and downstream samples are plotted in Fig. 2 with the summer hydrograph, which displays the hourly discharge rates (Q, m^3 s^{-1}) measured throughout the sampling period.
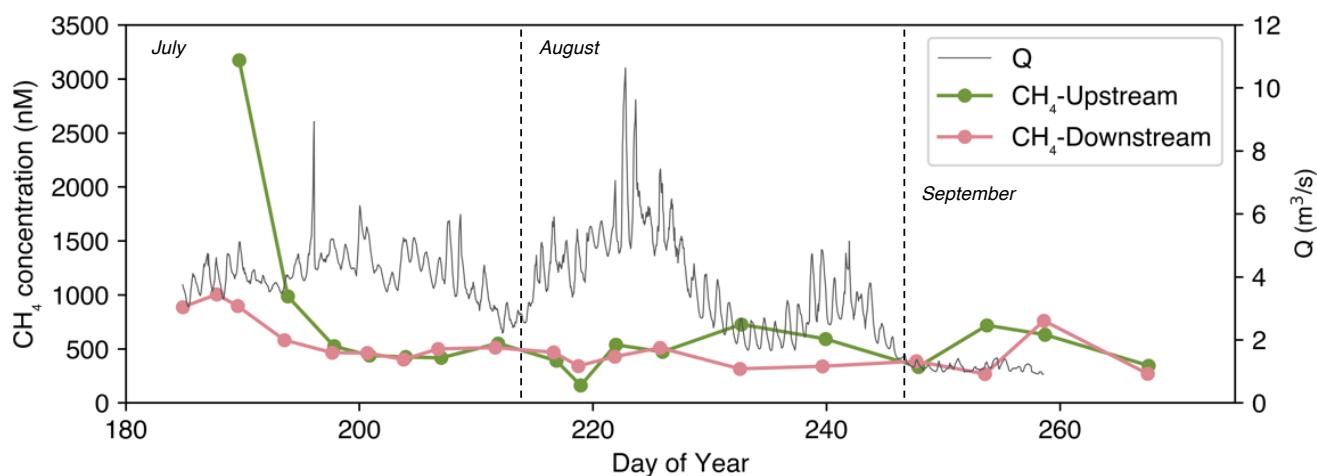
180

Figure 2. Measured methane concentrations (nM) of the upstream and downstream melt river plotted over the seasonal hydrograph, which provides hourly discharge measurements (Q) in m^3 s^{-1}.

Using the upstream methane concentrations throughout the summer and the discharge rates from the hydrograph, we calculate
185   the total amount of methane emerging from beneath the glacier within the melt river and the potential emissions. During the
monitoring period in 2021 (between 03 July and 23 September, 82 days), approximately 274 kg (217-342 kg) of methane were
transported from the glacier margin in the melt river, equating to an overall average of 3.34 kg per day. This amount does not
account for the amount of methane transported during the early melt season, prior to the monitoring period, or the end of the
melt season, after the monitoring period. Inferring early (26 May-02 July) and late season (24 September-06 October) discharge
190   rates through temperature-discharge correlations suggests that the methane flux throughout June and early October could add
an additional 345 kg (269-426 kg) of methane. Therefore, the total amount of methane transported by the melt river during the
full melt season is 618 kg (486-768 kg), and when considering the atmospheric equilibrium concentration, this translates to
potential methane emissions of 616 kg methane (484-766 kg).

3.1.1 Transect of the melt river

195   A one-time transect of samples was taken along the melt river in August 2022, starting at the two rivers feeding the melt river
(subglacial and supraglacial) and finishing at the fjord. The methane concentrations along this transect are shown in Fig. 3.
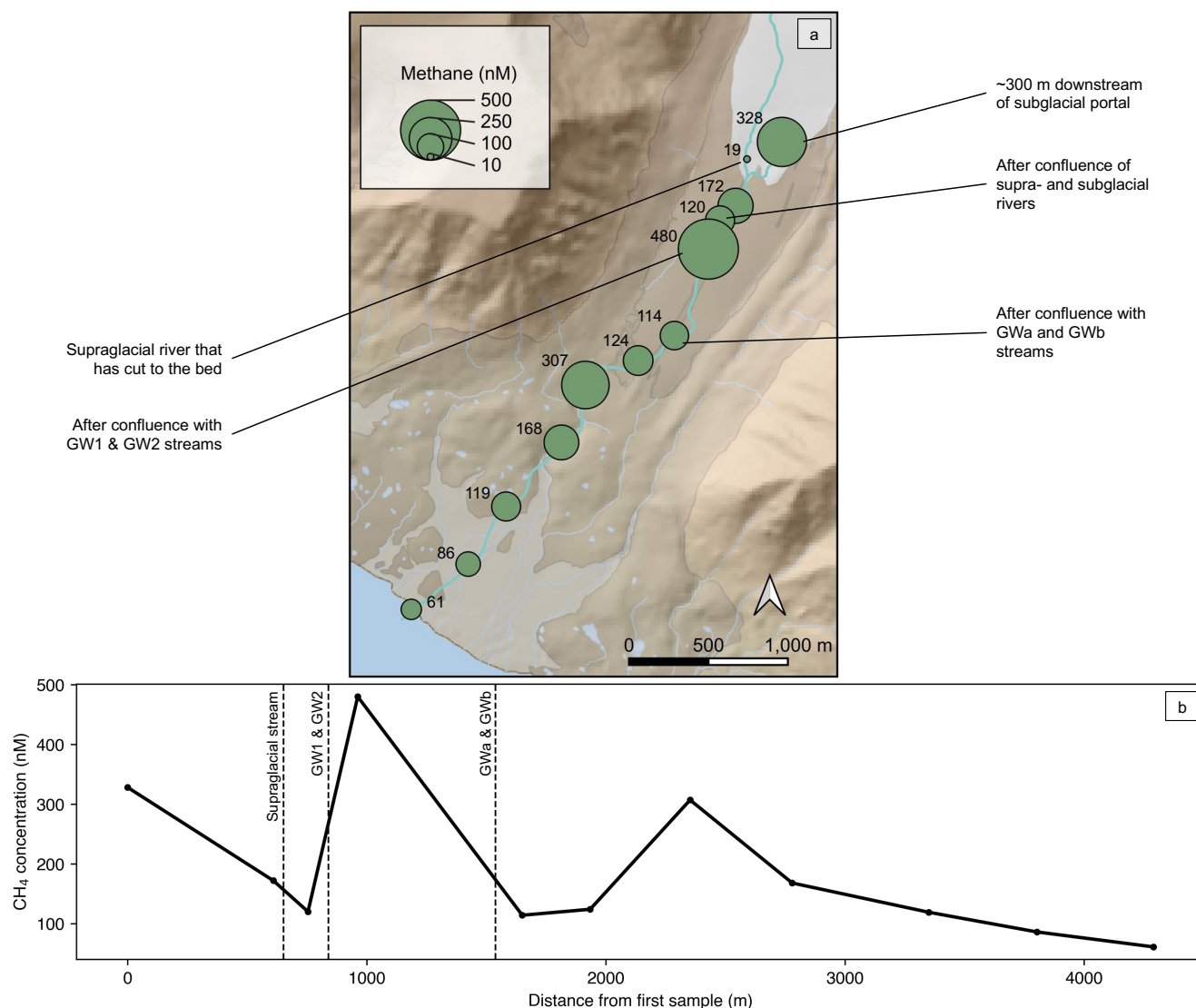
Figure 3. (a) Transect of methane concentrations (nM) of the melt river taken on 27 August 2022. Bubble size is correlated with methane concentration, according to the legend. (b) Methane concentrations (nM) plotted against distance river has flowed from the first sampling point. Vertical dashed lines represent confluence points with other streams.

3.2 Potential methane emissions from GW1 and GW2

Average discharge rates for GW1 and GW2 were used to calculate potential emissions. The outflow rates of the GW1 and GW2 springs were largely constant throughout the summers, averaging 1.1 L s^{-1} (± 0.19 L s^{-1}) and 0.86 L s^{-1} (± 0.18 L s^{-1}), respectively. Methane concentrations previously published for the GW1 and GW2 springs (Kleber et al., 2024), plotted in Fig. 4, are used to calculate potential methane emissions from the two groundwater sources. Seeing as the methane concentration

9

of the GW1 spring does not fluctuate much over the course of the melt season, potential methane emissions from the GW1 spring are calculated using the average concentration over the season and equate to 244 kg methane (99-150 kg). On the other hand, the methane concentrations of the GW2 spring vary considerably over the season. Therefore, linear interpolation between

210 the measured methane concentrations throughout the summer is used to estimate methane emissions from the spring and yields 115 kg CH_4 (70.8-164 kg) throughout the melt season.
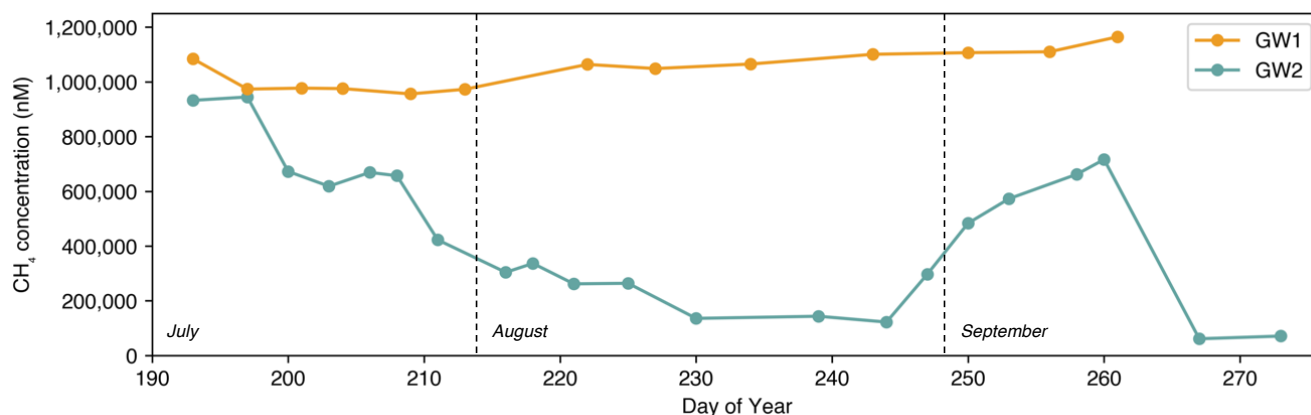
Figure 4. Methane concentrations of the GW1 and GW2 springs as reported in Kleber et al. (2024). The GW1 and GW2
215 **measurements were taken in 2022 and 2021, respectively.**

3.2.1 Transects of GW1 and GW2 outflows

Measurements of methane concentrations were made in transects along the outflow streams of the two groundwater springs. The results show an average decrease in methane of 29% ($n = 6$ transects) from the outflow of the GW2 spring to where the

220 stream meets a melt river, approximately 6 m away (Fig. 5a). The δ^{13}C-CH_4 shows no significant change or trend across the sampled transects and ranges from -44.6‰ to -42.5‰ (Fig. 5b). The transect of methane concentrations along the outflow of GW1 show an average decrease in methane of 78% ($n = 2$ transects) within 25 m downstream of the spring outlet (Fig. 5c). In contrast to the GW2 outlet, the δ^{13}C-CH_4 in the GW1 outlet becomes more enriched in ^{13}C as the methane concentration decreases across the sampled transects (Fig. 5d). In both transects, the δ^{13}C-CH_4 starts at -44.1‰ at the stream outflow and is

225 progressively enriched to -42.5‰ and -42.9‰ for each transect respectively at a point 25 m downstream.
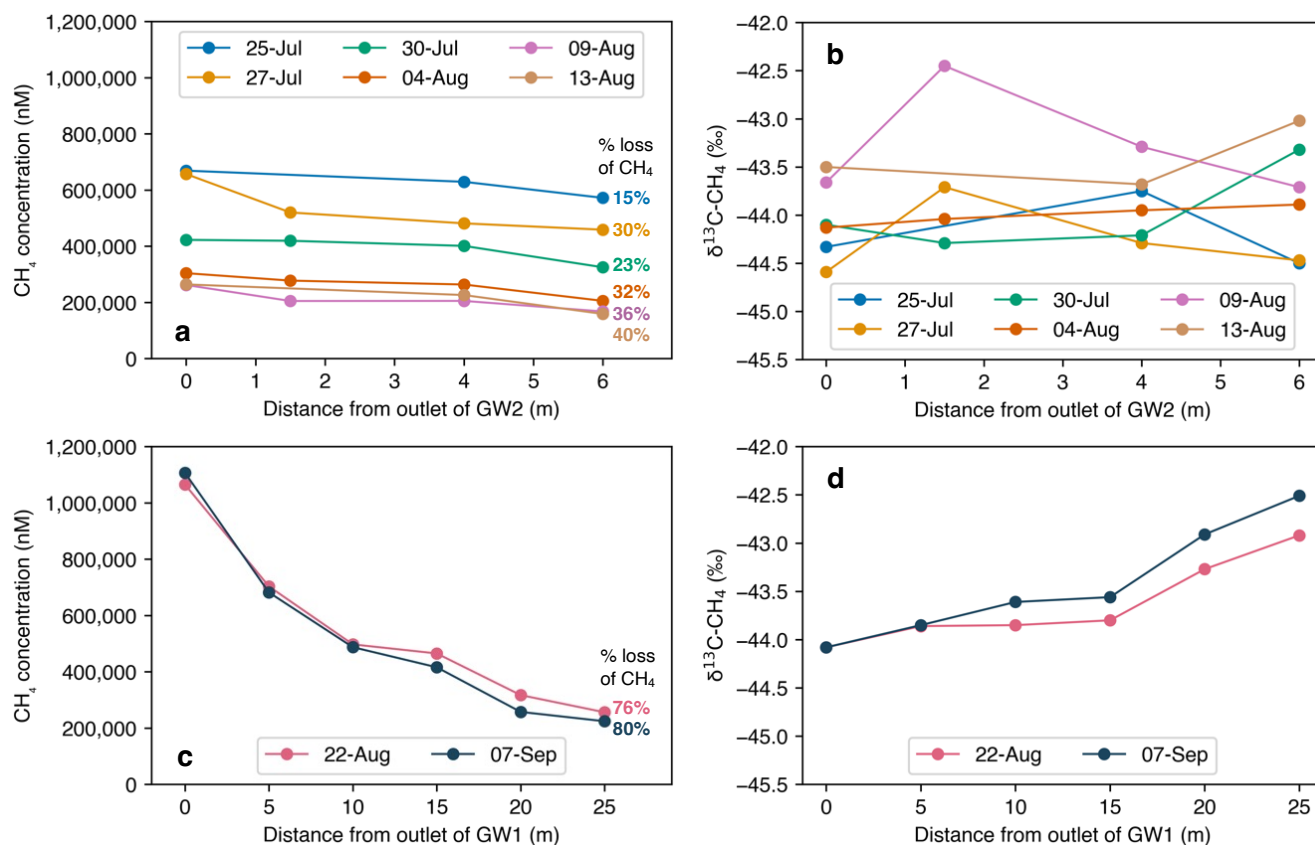
Figure 5. (a) Decrease of methane concentrations (nM) along the outflow of the GW2 spring, including the percent loss of methane across the full length of the transect. **(b)** Change in stable carbon isotopic composition ($\delta^{13}C$) of methane along the outflow of the GW2 spring. **(c)** Decrease of methane concentrations (nM) along the outflow of the GW1 spring, including the percent loss of methane across the full length of the transect. **(d)** Change in stable carbon isotopic composition of methane along the outflow of the GW1 spring.

3.2.2 Spatial variability in groundwater methane concentrations

Spatial sampling of groundwaters throughout the glacial forefield was undertaken during the summer of 2021. Waters collected from 14 additional groundwater springs located between the glacier margin and the fjord revealed more springs that are super-saturated with methane (Fig. 6). Methane concentrations of the other groundwaters range from below the detection limit (<18 nM) to 73,300 nM, with the two highest concentration springs at 25,200 nM and 73,300 nM and hereafter referred to as GWa and GWb, respectively.

11
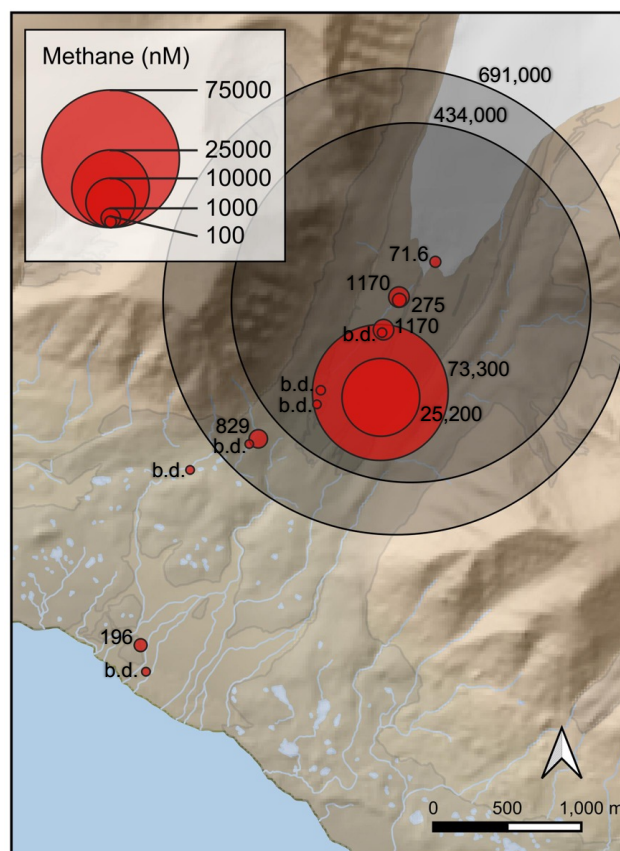
Figure 6. Methane concentrations (nM) of groundwater springs in the forefield of Vallåkrabreen. Bubble size is proportional to methane concentration. Red bubbles represent springs sampled during one-time spatial sampling, while black bubbles represent the average methane concentrations of the GW1 and GW2 springs (Kleber et al., 2024), with bubble size extrapolated on the same bubble size scale. Concentrations below the detection limit of 18 nM are indicated by b.d.

3.3 Methane ebullition

Ebullition from vents at the bed of groundwater pools and the bed of the groundwater streams was observed nearly constantly throughout the summer field seasons. During the summer of 2021, approximately ten vents were observed across five groundwater pools that regularly released small plumes of bubbles. Average ebullition rates measured from five of these vents range from 1.2 to 3.9 L hr^{-1} (average: 2.6 L hr^{-1}). It was not possible to measure the release rates of most of the visible vents due to water that was too shallow for the bubble trap. Analysis of the gas, which readily ignited with a lighter when collected in the field, revealed an average methane concentration of 350,000 ppm (ranging from 254,000 to 482,000 ppm, $n = 9$).

4 Discussion

The potential methane emissions from each hydrological system of the Vallåkrabreen catchment (melt river and groundwater) have been derived using a simple mass balance approach. This approach describes the amount of methane exceeding the

255 atmospheric equilibrium concentration that is transported to the proglacial area and therefore has the potential to be released to the atmosphere. We use this method to avoid the large uncertainties that can be attributed to small uncertainties in predicting a gas transfer velocity (or k-value) (Wanninkhof, 1992). The dynamic nature of the glacial melt river means that the characteristics used to predict a k-value, including discharge, channel geometry and velocity (Raymond et al., 2012) vary greatly throughout the season. Furthermore, frequent additional sources of methane to the river, as observed in Fig. 3, preclude

260 the use of mass balance to define a k-value for the main river. In the following sections, we discuss the accuracy of the potential emissions and consider the likelihood of any methane oxidation in each of the hydrological systems.

4.1 Methane emissions from the melt river

Potential emissions from the melt river are estimated at 616 kg methane (484-766 kg) over the melt season (when considering the atmospheric equilibrial concentration of ~4 nM methane that remains in the water). We suspect that the methane in the

265 melt river is largely unaltered by biological processes within the river and thus the microbial oxidation of methane is negligible compared to physical loss driven by the river's turbulence. This is a reasonable assumption based on previous studies (e.g. Bussmann, 2013; Lilley et al., 1996; Rovelli et al., 2022). We also assume that the methane measured in the melt river at the upstream sampling point has sufficient time to degas along the ~4.5 km before the river reaches the fjord. Methane is a poorly soluble gas and its transfer velocity has been found to increase exponentially with turbulence (Herlina and Jirka, 2008), thus

270 it is expected that the methane degases rapidly from the highly turbulent river. We observe rapid losses of methane from the river in Fig. 3, where 76% of the methane is lost within a stretch of 650 m.

The calculated potential emissions are conservative because they do not account for the methane that was degassed prior to the upstream sampling point, such as within low pressure channels at the glacier bed (e.g. Christiansen and Jørgensen, 2018).

275 In addition, samples for the measurement of methane concentration were taken at a point approximately 50 m downstream of where the main melt river emerged from a glacial cave at the start of summer. The cave, however, gradually collapsed throughout the season, and thus the point where the river emerged from the cave moved upstream by several hundred meters by the end of the summer. The sampling point was kept constant, which means that as the summer progressed, the river had more contact time with the atmosphere before the samples were taken. Therefore, the measured methane concentrations are

280 presumably much lower than the actual values in the water emerging directly from the subglacial portal due to degassing before reaching the sampling point. This may have a significant effect on the calculated emission rate, yielding a lower value than reality.

285 High methane concentrations in the melt river at the beginning of summer are likely due to an accumulation of methane beneath the glacier during winter, which is then transported out along the drainage system as the river begins to flow at the start of the melt season. It is important to note that due to the difficulty of accessing the site during the onset of the melt season, the earliest samples of this study were taken more than a month after the river would have started flowing. Therefore, the river likely had considerably higher methane concentrations during May and June before the sampling period of this study began, and there may be a considerable amount of methane not captured in our emission estimate.

290

Regardless, this emission rate is substantial considering the size of Vallåkrabreen (~20 km^2). The Leverett Glacier, a ~600 km^2 outlet glacier of the Greenland Ice Sheet, has been estimated to transport between 2.78 and 6.28 t of methane from its subglacial catchment to the glacier margin over an entire melt season (Lamarche-Gagnon et al., 2019). At only 3% the size, Vallåkrabreen's river may be conveying up to 28% of the methane estimated for the melt river at Leverett Glacier.

295

The concentrations of methane at the downstream sampling site of the melt river are not always lower than the upstream values, as would be expected from continued degassing of methane from the river as it flows downstream. This is likely the result of additional methane sources, such as groundwater streams, entering the river along its flowpath and supplying additional methane to the stream. Figure 3 shows a transect of dissolved methane concentrations measured along the melt river, starting
300 as close to where the main river emerged from the glacier cave as possible (about 300 m downstream) and finishing where the river met the fjord (about 4 km downstream). Considerable increases in methane concentrations at points along the stream suggest several additional sources of methane to the river. The most notable one is where the GW1 and GW2 springs join the melt river, increasing the river's methane concentration from 120 nM about 150 m upstream of the confluence, to 480 nM about 200 m downstream of the confluence. It appears that additional methane sources continue to enter the river throughout
305 the moraine, until the river reaches the large flood plain before the fjord, where it continually loses methane during the last 1300 m.

4.2 Methane emissions from groundwater outflow streams

4.2.1 GW1 spring

Transect samples of the GW1 outflow indicate rapid loss of methane from the water after it emerges from the spring, likely
310 enhanced by the turbulence of flowing water (Fortescue and Pearson, 1967). Losses of methane of up to 80% were observed within the first 25 m of the GW1 outflow stream (Fig. 5c), with corresponding changes in the carbon isotopic composition of the methane remaining in the stream (Fig. 5d). An enrichment in the heavier ^{13}C isotope suggests that methane is being oxidized in the groundwater, preferentially consuming molecules containing the lighter ^{12}C isotope. Kinetic isotopic fractionation of methane during degassing from water is very small (Knox et al., 1992) and likely negligible at such high concentrations,
315 whereas significant carbon isotope fractionation can occur during microbial oxidation reactions of methane, including during

microbially-mediated methanotrophy (Whiticar, 1999). While the physical loss of methane via degassing from the stream is still occurring, methanotrophy is an active methane sink within the GW1 outflow, consuming some of the methane before it is lost to the atmosphere.

320   Therefore, the 244 kg (99-150 kg) of potential emissions calculated from the GW1 spring is too high, as the consumption of methane due to methanotrophy along the outflow stream must be considered to estimate actual emissions. Although microbial oxidation is clearly active in the outflow, it is not expected that the rates are exceptionally high. The low temperature of the water (~0°C) will reduce the rate of all biological activity, including methanotrophy (Lofton et al., 2014). Furthermore, the carbon isotopic composition of the methane increases only slightly (by 1.2-1.6‰) whilst the concentration of methane in the

325   stream decreases by nearly 80%, suggesting that methanotrophy is not the dominant process contributing to the loss of methane from the stream.

Using a closed-system Rayleigh function (Equation 3) (Whiticar, 1999), we can calculate the percent of methane possibly lost due to methanotrophy:

330    $$\delta^{13}C_{CH_{4,t}} = \delta^{13}C_{CH_{4,i}} + \varepsilon \ln(1 - F), \qquad (4)$$

where $\delta^{13}C_{CH_{4,t}}$ is the carbon isotope ratio of the methane remaining in the stream at time t, $\delta^{13}C_{CH_{4,i}}$ is the carbon isotope ratio of the initial methane in the stream outflow prior to oxidation, ε is the magnitude of the carbon isotope fractionation during methane oxidation between the outflow of the stream and t, and F is the fraction of methane lost during this time.

335   The magnitudes of carbon isotopic fractionation (ε) typically measured during methanotrophy range from 5 to 31 (Whiticar, 1999). Using the change in carbon isotopic composition over the length of the transect and the typical magnitudes of isotopic fractionation due to methanotrophy, we find that the loss of methane due to methanotrophy should be a maximum of 26.1% on 27 August and 36.9% on 07 September 2022 (Fig. 7). Therefore, methanotrophy could only account for a small portion of the observed methane loss over the length of the transect—anywhere from 5.0 to 34% on 27 August and 6.5 to 46% on 07
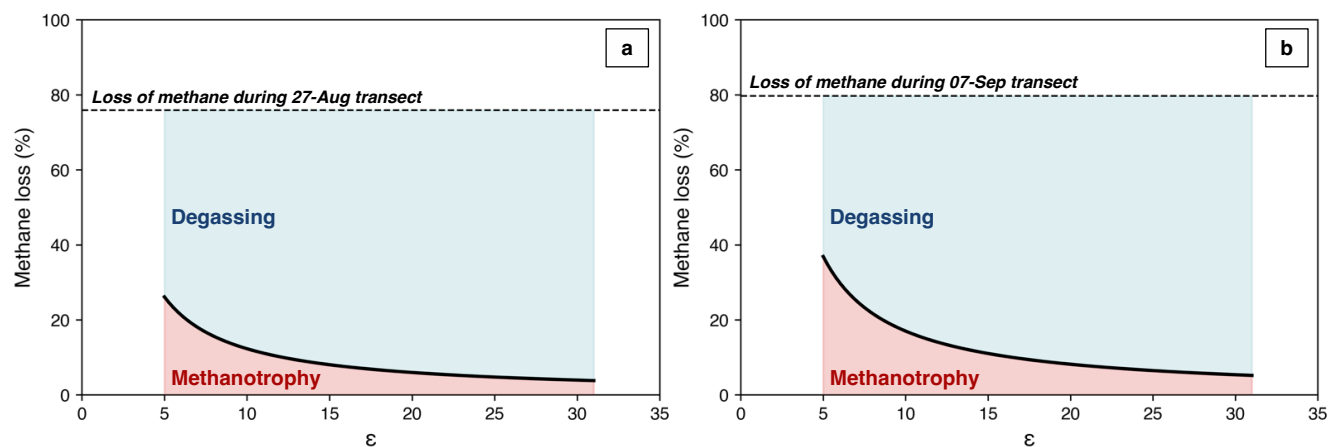
340   September.

Figure 7. Range of expected methane loss due to methanotrophy on (a) 27 August 2022 and (b) 7 September 2022. Percent methane loss is calculated with Equation 3, using the measured carbon isotopic compositions for $\delta^{13}C_{CH_{4,t}}$ and $\delta^{13}C_{CH_{4,i}}$ from the overall transect and using the range of magnitudes of isotope fractionation (ε) typically measured during methanotrophy (5-31). The range of methane loss due to methanotrophy is shaded pink and the balance due to degassing is shaded blue. The measured percent of methane lost across the whole transect is indicated by the dashed line in each plot.

Heilweil et al. (2016) used gas-tracer experiments to determine the relative contributions of degassing and in-stream oxidation to methane-loss from small streams, which yielded a degassing/microbial oxidation ratio of 6:1. Since it's not possible to calculate the contribution of methanotrophy to the reduction of methane in the GW1 outflow with our available data, we use this ratio to estimate and, in turn, determine the amount of methane likely to be degassed. This ratio suggests that 14% of the methane lost across the length of the transect is lost due to methanotrophy. This percentage fits conservatively within the ranges calculated in Fig. 7. Therefore, assuming 14% of the methane in the GW1 spring is microbially oxidized within the water column of the outflow stream, actual methane emissions due to degassing from the GW1 spring are likely to be 210 kg CH4 (125-289 kg) across the melt season.

4.2.2 GW2 spring

Transect samples of the GW2 outflow stream show significant losses of methane, up to 40%, over a relatively short distance (~6 m). There were no significant changes observed in the carbon isotopic composition of the remaining methane along the transects. There were also no additional inputs of water into this section of the stream and therefore no chance for dilution along the flowpath. This suggests that degassing of methane to the atmosphere accounts for its rapid decline from the water rather than it being diluted or microbially oxidized within the water.

The rate of methane evasion from a river due to degassing can be much faster than that of microbial oxidation (Heilweil et al., 2016; Rovelli et al., 2022), especially in smaller streams where the depth is shallow and the surface-area-to-volume ratios are

16

365 large. Thus, it is assumed that the rate of removal of methane from the water due to methanotrophy, if any, is negligible relative to the rate at which it degasses to the atmosphere. Consequently, we believe that the potential emission rate calculated for the GW2 spring, 115 kg CH_4 (70.8-164 kg) throughout the melt season, is a reasonable estimate for its actual emissions.

4.2.3 GWa and GWb springs

Spatial sampling of other groundwaters throughout the glacial forefield revealed additional springs that are super-saturated with methane (Fig. 6). Most of the saturation levels of these groundwaters are much lower than those observed in the GW1
370 and GW2 springs, suggesting that most of the groundwater methane emissions within the forefield are released from localized hotspots. Two of the springs, GWa and GWb, which are located within 50 m of each other, contain substantial amounts of methane (25,100 nM and 73,300 nM, respectively). This area likely represents another emission hotspot. Assuming their discharge rates are approximately 0.97 L s^{-1} (the average of GW1 and GW2 discharge rates)—a reasonable assumption considering their similar size—the two springs may release up to 20.3 kg CH_4 (12.6-29.2 kg) throughout the melt season
375 combined. Evasion of methane from some of the less concentrated springs is certainly occurring, as many have levels significantly above the concentration at equilibrium with the atmosphere, however these emissions are likely to be less than a few kilograms per summer and thus comparatively negligible.

4.3 Methane ebullition from groundwater pools

Ebullition within the groundwater pools and outflows was observed nearly constantly. Assuming an average release rate of 2.6
380 L hr^{-1} of gas from 10 vents at any given time throughout the summer, total ebullition emissions are estimated as 24.0 kg CH_4 (20.9-27.1 kg) over the five months where the icing was not capping the groundwater springs (typically June through October). This is a conservative estimate, as there are likely to have been more active vents in other groundwater pools or springs that were not observed. Only 10 vents were assumed in the calculations because only 10 vents were observed to emit bubbles on a regular basis (observed at each visit to the groundwater springs) and were in deep enough water to measure the rate of
385 ebullition. However, many more vents were observed that emitted bubbles sporadically and these were not accounted for. In addition, a chamber measurement over a dry vent (in a groundwater pool that had drained) confirmed that the vent was still active even after the inflow of groundwater had ceased (Supplementary Fig. S.4). Ambient methane concentration within the chamber increased rapidly to nearly 5000 ppm during one of the 15-minutes increments of the 45-minute monitoring period. Therefore, there are likely additional vents throughout the forefield that are no longer coupled to active groundwater pools and
390 thus difficult to identify in the field.

4.4 Total methane emission estimate

The total estimate of melt season emissions from the Vallåkrabreen catchment equates to 1.0 ton of methane (± 0.3 ton) between June and October. Methane emissions from the glacial melt river are projected to contribute 63% of these emissions, while the groundwater and ebullition contribute 35% and 2%, respectively.

395

This melt-season emission estimate is conservative due to various limitations in the field—most notably, the inability of sampling all groundwater springs in the catchment and the inaccessibility of the melt river directly at the glacier margin. The impracticality of identifying and measuring all groundwater springs throughout the forefield makes it likely that there are methane-rich springs that we are unaware of and are therefore not accounted for in our emissions estimate. This is apparent in

400 the notable increase of methane in the melt river transect from 124 to 307 nM (Fig. 3) in an area where a groundwater spring had not been identified. The inability of accessing the melt river at the glacier margin means that methane was lost from the river before the methane concentrations were measured at the upstream sampling point. The methane degassed between the margin and the sampling point (a distance ranging from ~50-200 m throughout the summer) could be substantial considering the high turbulence of the river and the rapid loss of methane observed in the river transect in Fig. 3. This may represent a

405 considerable amount of methane not accounted for in our emissions estimate.

4.5 Methane source

While the methane in the groundwater of the Vallåkrabreen catchment has previously been found, through isotopic analysis, to be geologically sourced (Kleber et al., 2024), it is difficult to constrain the origin of the methane detected in the glacial melt river. Methane concentrations in the river were not high enough for analysis of the stable carbon isotopic composition with the

410 instruments available, which could have indicated if the methane was ancient geologic methane or more contemporarily produced microbial methane. Previous studies have suggested that microbial methane production can occur in subglacial environments due to the considerable amounts of organic carbon that can be sequestered during a glacier's advance and the presence of anoxic conditions (Boyd et al., 2010; Burns et al., 2018; Dieser et al., 2014; Stibal et al., 2012; Wadham et al., 2008). It has been widely agreed in studies of methane-emitting glacial rivers across the Arctic and sub-Arctic that subglacial

415 methane is largely microbially produced (Burns et al., 2018; Christiansen et al., 2021; Lamarche-Gagnon et al., 2019; Pain et al., 2020).

The potential for methanogenesis in the subglacial environment, however, has been found to depend largely on the sediment type and, in turn, the character of the organic substrate and its bioavailability (O'Donnell et al., 2016; Stibal et al., 2012). The

420 rates of methane production within various subglacial sediment types have been found to vary by orders of magnitude (Stibal et al., 2012). O'Donnell et al. (2016) compared the abundance and availability of organic carbon in sediments in basal ice from glaciers overriding different substrates. They found that the Finsterwalderbreen glacier, the only Svalbard glacier in the study, which is situated less than 60 km southwest of Vallåkrabreen, contained the least amount of bioavailable organic compounds within its basal ice—an order of magnitude lower than Joyce Glacier in Antarctica, which had overridden a lacustrine

425 environment. The dissolved organic carbon present in the basal ice of Finsterwalderbreen is thought to be mainly derived from kerogen in the bedrock, which has limited bioreactivity (Wadham et al., 2004). Considering Vallåkrabreen is situated in a

18

similar geological and geographical setting to Finsterwalderbreen, it is expected that the basal sediments of the Vallåkrabreen catchment would offer similarly low levels of organic substrates to stimulate microbial activity.

430   Ultimately, while some methanogenesis is potentially occurring in the subglacial environment of Vallåkrabreen, we hypothesize that any microbially-produced methane in the drainage system is supplemented largely by thermogenic methane sourced from the rocks over which the glacier has flowed. The physical processes related to glacial advance—such as the excavation of large depths of bedrock through glacial erosion and geological faulting induced by glacial loading—can encourage the migration of deep-seated hydrocarbons to the surface where they may be introduced to the subglacial drainage
435   system (Patton et al., 2022; Vachon et al., 2022). Alternatively, pressurized subglacial water may route through the fractured bedrock beneath the glacier, extracting methane along its flowpath—effectively inducing a natural 'glacial fracking' process. Furthermore, methane-rich groundwater springs that bring deep-seated methane to the surface may enter the subglacial river before it emerges from the glacier terminus, providing a source of concentrated geologic methane to the river water.

440   Our study shows that small valley glaciers like Vallåkrabreen can be a substantial source of methane, challenging previous theories that subglacial methane is largely produced microbially in the anoxic environment beneath large ice sheets (Wadham et al., 2008). Vallåkrabreen is one of more than 1400 land-terminating glaciers on Svalbard (Nuth et al., 2013), many flowing over geology that is rich in organic carbon, such as shale, coal and sandstone. We suspect that emissions from methane-rich glacial rivers on Svalbard are prevalent across the archipelago and may amount to a large, seasonal source of methane to the
445   region's atmosphere. Our findings suggest that methane emissions from glacial rivers is likely more widespread than previously thought, and contributions from valley and mountain glaciers across the Arctic should not be discounted.

5 Conclusions

Glacial groundwater on Svalbard is known to bring deep-seated geologic methane to the surface in glacier forefields and is a considerable source of methane to the region's atmosphere (Kleber et al., 2023). Methane emissions from glacial melt rivers,
450   on the other hand, have previously not been considered on Svalbard. Our temporal investigations into methane dynamics in the Vallåkrabreen catchment during the melt season reveal that the glacial melt river flushes significant amounts of methane from beneath the glacier and into the pro-glacial area. While we identify several hotspots of exceptionally methane-super-saturated groundwater seepage throughout the forefield, the glacial melt river nevertheless accounts for nearly two-thirds of the conservatively estimated 1.0 t of total melt season methane emissions. Our findings highlight that glacier forefields on
455   Svalbard are hotspots for methane emissions. This study represents the first account of methane emissions associated to glacial melt rivers on Svalbard and indicates that they may represent a significant source of regional methane emissions that are currently overlooked.

Data availability

All raw data can be provided by the corresponding authors upon request.

460 **Supplement**

The supplement related to this article is available online at: TBD

Author contributions

GEK and AH designed the study. GEK and LM conducted the fieldwork. GEK performed the laboratory analysis with support from MT and YZ. GEK analyzed the data and drafted the manuscript. LM, AVT, MT and AH reviewed and edited the 465 manuscript.

Competing interests

The authors declare that they have no conflict of interest.

Disclaimer

Publisher's note: Copernicus Publications remains neutral with regard to jurisdictional claims made in the text, published 470 maps, institutional affiliations, or any other geographical representation in this paper. While Copernicus Publications makes every effort to include appropriate place names, the final responsibility lies with the authors.

References

480 Abay, T. b., Karlsen, D. a., Lerch, B., Olaussen, S., Pedersen, J. h., Backer-Owe, K., 2017. Migrated Petroleum in Outcropping Mesozoic Sedimentary Rocks in Spitsbergen: Organic Geochemical Characterization and Implications for Regional Exploration. Journal of Petroleum Geology 40, 5–36. https://doi.org/10.1111/jpg.12662

Boyd, E.S., Skidmore, M., Mitchell, A.C., Bakermans, C., Peters, J.W., 2010. Methanogenesis in subglacial sediments. Environmental Microbiology Reports 2, 685–692. https://doi.org/10.1111/j.1758-2229.2010.00162.x

Burns, R., Wynn, P.M., Barker, P., McNamara, N., Oakley, S., Ostle, N., Stott, A.W., Tuffen, H., Zhou, Z., Tweed, F.S.,
485 Chesler, A., Stuart, M., 2018. Direct isotopic evidence of biogenic methane production and efflux from beneath a temperate glacier. Sci Rep 8, 17118. https://doi.org/10.1038/s41598-018-35253-2

Bussmann, I., 2013. Distribution of methane in the Lena Delta and Buor-Khaya Bay, Russia. Biogeosciences 10, 4641–4652. https://doi.org/10.5194/bg-10-4641-2013

Christiansen, J.R., Jørgensen, C.J., 2018. First observation of direct methane emission to the atmosphere from the subglacial
490 domain of the Greenland Ice Sheet. Sci Rep 8, 16623. https://doi.org/10.1038/s41598-018-35054-7

Christiansen, J.R., Röckmann, T., Popa, M.E., Sapart, C.J., Jørgensen, C.J., 2021. Carbon Emissions From the Edge of the Greenland Ice Sheet Reveal Subglacial Processes of Methane and Carbon Dioxide Turnover. JGR Biogeosciences 126. https://doi.org/10.1029/2021JG006308

Dieser, M., Broemsen, E.L.J.E., Cameron, K.A., King, G.M., Achberger, A., Choquette, K., Hagedorn, B., Sletten, R., Junge,
495 K., Christner, B.C., 2014. Molecular and biogeochemical evidence for methane cycling beneath the western margin of the Greenland Ice Sheet. ISME J 8, 2305–2316. https://doi.org/10.1038/ismej.2014.59

Fortescue, G.E., Pearson, J.R.A., 1967. On gas absorption into a turbulent liquid. Chemical Engineering Science 22, 1163–1176. https://doi.org/10.1016/0009-2509(67)80183-0

Gautier, D.L., Bird, K.J., Charpentier, R.R., Grantz, A., Houseknecht, D.W., Klett, T.R., Moore, T.E., Pitman, J.K., Schenk,
500 C.J., Schuenemeyer, J.H., Sørensen, K., Tennyson, M.E., Valin, Z.C., Wandrey, C.J., 2009. Assessment of Undiscovered Oil and Gas in the Arctic. Science 324, 1175–1179. https://doi.org/10.1126/science.1169467

Heilweil, V.M., Solomon, D.K., Darrah, T.H., Gilmore, T.E., Genereux, D.P., 2016. Gas-Tracer Experiment for Evaluating the Fate of Methane in a Coastal Plain Stream: Degassing versus in-Stream Oxidation. Environ. Sci. Technol. 50, 10504–10511. https://doi.org/10.1021/acs.est.6b02224

505 Herlina, Jirka, G.H., 2008. Experiments on gas transfer at the air–water interface induced by oscillating grid turbulence. J. Fluid Mech. 594, 183–208. https://doi.org/10.1017/S0022112007008968

Hodson, A.J., Nowak, A., Redeker, K.R., Holmlund, E.S., Christiansen, H.H., Turchyn, A.V., 2019. Seasonal Dynamics of Methane and Carbon Dioxide Evasion From an Open System Pingo: Lagoon Pingo, Svalbard. Front. Earth Sci. 7, 30. https://doi.org/10.3389/feart.2019.00030

510 Hugelius, G., Strauss, J., Zubrzycki, S., Harden, J.W., Schuur, E.A.G., Ping, C.-L., Schirrmeister, L., Grosse, G., Michaelson, G.J., Koven, C.D., O'Donnell, J.A., Elberling, B., Mishra, U., Camill, P., Yu, Z., Palmtag, J., Kuhry, P., 2014. Estimated stocks of circumpolar permafrost carbon with quantified uncertainty ranges and identified data gaps. Biogeosciences 11, 6573–6593. https://doi.org/10.5194/bg-11-6573-2014

Isaksen, I.S.A., Gauss, M., Myhre, G., Walter Anthony, K.M., Ruppel, C., 2011. Strong atmospheric chemistry feedback to
515 climate warming from Arctic methane emissions. Global Biogeochemical Cycles 25. https://doi.org/10.1029/2010GB003845

Kleber, G.E., Hodson, A.J., Magerl, L., Mannerfelt, E.S., Bradbury, H.J., Zhu, Y., Trimmer, M., Turchyn, A.V., 2023. Groundwater springs formed during glacial retreat are a large source of methane in the high Arctic. Nat. Geosci. 16, 597–604. https://doi.org/10.1038/s41561-023-01210-6

520 Kleber, G.E., Magerl, L., Turchyn, A.V., Redeker, K., Thiele, S., Liira, M., Herodes, K., Øvreås, L., Hodson, A., 2024. Shallow and deep groundwater moderate methane dynamics in a high Arctic glacial catchment. Frontiers in Earth Science 12.

Knox, M., Quay, P.D., Wilbur, D., 1992. Kinetic isotopic fractionation during air-water gas transfer of O2, N2, CH4, and H2. Journal of Geophysical Research: Oceans 97, 20335–20343. https://doi.org/10.1029/92JC00949

Lamarche-Gagnon, G., Wadham, J.L., Sherwood Lollar, B., Arndt, S., Fietzek, P., Beaton, A.D., Tedstone, A.J., Telling, J.,
525 Bagshaw, E.A., Hawkings, J.R., Kohler, T.J., Zarsky, J.D., Mowlem, M.C., Anesio, A.M., Stibal, M., 2019.

        Greenland melt drives continuous export of methane from the ice-sheet bed. Nature 565, 73–77. https://doi.org/10.1038/s41586-018-0800-0

Lilley, M.D., de Angelis, M.A., Olson, E.J., 1996. Methane concentrations and estimated fluxes from Pacific Northwest rivers. SIL Communications, 1953-1996 25, 187–196. https://doi.org/10.1080/05384680.1996.11904080

530   Lofton, D.D., Whalen, S.C., Hershey, A.E., 2014. Effect of temperature on methane dynamics and evaluation of methane oxidation kinetics in shallow Arctic Alaskan lakes. Hydrobiologia 721, 209–222. https://doi.org/10.1007/s10750-013-1663-x

McGuire, A.D., Anderson, L.G., Christensen, T.R., Dallimore, S., Guo, L., Hayes, D.J., Heimann, M., Lorenson, T.D., Macdonald, R.W., Roulet, N., 2009. Sensitivity of the carbon cycle in the Arctic to climate change. Ecological
535   Monographs 79, 523–555. https://doi.org/10.1890/08-2025.1

Nuth, C., Kohler, J., König, M., von Deschwanden, A., Hagen, J.O., Kääb, A., Moholdt, G., Pettersson, R., 2013. Decadal changes from a multi-temporal glacier inventory of Svalbard. The Cryosphere 7, 1603–1621. https://doi.org/10.5194/tc-7-1603-2013

O'Donnell, E.C., Wadham, J.L., Lis, G.P., Tranter, M., Pickard, A.E., Stibal, M., Dewsbury, P., Fitzsimons, S., 2016.
540   Identification and analysis of low-molecular-weight dissolved organic carbon in subglacial basal ice ecosystems by ion chromatography. Biogeosciences 13, 3833–3846. https://doi.org/10.5194/bg-13-3833-2016

Pain, A.J., Martin, J.B., Martin, E.E., Rahman, S., 2020. Heterogenous CO_2 and CH_4 content of glacial meltwater of the Greenland Ice Sheet and implications for subglacial carbon processes. The Cryosphere Discussions 1–33. https://doi.org/10.5194/tc-2020-155

545   Patton, H., Hubbard, A., Heyman, J., Alexandropoulou, N., Lasabuda, A.P.E., Stroeven, A.P., Hall, A.M., Winsborrow, M., Sugden, D.E., Kleman, J., Andreassen, K., 2022. The extreme yet transient nature of glacial erosion. Nat Commun 13, 7377. https://doi.org/10.1038/s41467-022-35072-0

Rantanen, M., Karpechko, A.Y., Lipponen, A., Nordling, K., Hyvärinen, O., Ruosteenoja, K., Vihma, T., Laaksonen, A., 2022. The Arctic has warmed nearly four times faster than the globe since 1979. Commun Earth Environ 3, 1–10.
550   https://doi.org/10.1038/s43247-022-00498-3

Raymond, P.A., Zappa, C.J., Butman, D., Bott, T.L., Potter, J., Mulholland, P., Laursen, A.E., McDowell, W.H., Newbold, D., 2012. Scaling the gas transfer velocity and hydraulic geometry in streams and small rivers. Limnology and Oceanography: Fluids and Environments 2, 41–53. https://doi.org/10.1215/21573689-1597669

Rovelli, L., Olde, L.A., Heppell, C.M., Binley, A., Yvon-Durocher, G., Glud, R.N., Trimmer, M., 2022. Contrasting
555   Biophysical Controls on Carbon Dioxide and Methane Outgassing From Streams. Journal of Geophysical Research: Biogeosciences 127, e2021JG006328. https://doi.org/10.1029/2021JG006328

Sapper, S.E., Jørgensen, C.J., Schroll, M., Keppler, F., Christiansen, J.R., 2023. Methane emissions from subglacial meltwater of three alpine glaciers in Yukon, Canada. Arctic, Antarctic, and Alpine Research 55, 2284456. https://doi.org/10.1080/15230430.2023.2284456

560   Schuur, E. a. G., McGuire, A.D., Schädel, C., Grosse, G., Harden, J.W., Hayes, D.J., Hugelius, G., Koven, C.D., Kuhry, P., Lawrence, D.M., Natali, S.M., Olefeldt, D., Romanovsky, V.E., Schaefer, K., Turetsky, M.R., Treat, C.C., Vonk, J.E., 2015. Climate change and the permafrost carbon feedback. Nature 520, 171–179. https://doi.org/10.1038/nature14338

Schuur, E.A.G., Bockheim, J., Canadell, J.G., Euskirchen, E., Field, C.B., Goryachkin, S.V., Hagemann, S., Kuhry, P., Lafleur,
565   P.M., Lee, H., Mazhitova, G., Nelson, F.E., Rinke, A., Romanovsky, V.E., Shiklomanov, N., Tarnocai, C., Venevsky, S., Vogel, J.G., Zimov, S.A., 2008. Vulnerability of Permafrost Carbon to Climate Change: Implications for the Global Carbon Cycle. BioScience 58, 701–714. https://doi.org/10.1641/B580807

Stibal, M., Wadham, J.L., Lis, G.P., Telling, J., Pancost, R.D., Dubnick, A., Sharp, M.J., Lawson, E.C., Butler, C.E.H., Hasan, F., Tranter, M., Anesio, A.M., 2012. Methanogenic potential of Arctic and Antarctic subglacial environments with
570   contrasting organic carbon sources. Global Change Biology 18, 3332–3345. https://doi.org/10.1111/j.1365-2486.2012.02763.x

Turnipseed, D.P., Sauer, V.B., 2010. Discharge measurements at gaging stations (Report No. 3-A8), Techniques and Methods. Reston, VA. https://doi.org/10.3133/tm3A8

Vachon, R., Schmidt, P., Lund, B., Plaza-Faverola, A., Patton, H., Hubbard, A., 2022. Glacially Induced Stress Across the
575   Arctic From the Eemian Interglacial to the Present—Implications for Faulting and Methane Seepage. Journal of
Geophysical Research: Solid Earth 127, e2022JB024272. https://doi.org/10.1029/2022JB024272

Wadham, J.L., Bottrell, S., Tranter, M., Raiswell, R., 2004. Stable isotope evidence for microbial sulphate reduction at the bed
of a polythermal high Arctic glacier. Earth and Planetary Science Letters 219, 341–355.
https://doi.org/10.1016/S0012-821X(03)00683-6

580 Wadham, J.L., Tranter, M., Tulaczyk, S., Sharp, M., 2008. Subglacial methanogenesis: A potential climatic amplifier? Global
Biogeochemical Cycles 22. https://doi.org/10.1029/2007GB002951

Walter Anthony, K.M., Anthony, P., Grosse, G., Chanton, J., 2012. Geologic methane seeps along boundaries of Arctic
permafrost thaw and melting glaciers. Nature Geosci 5, 419–426. https://doi.org/10.1038/ngeo1480

Walter, K.M., Zimov, S.A., Chanton, J.P., Verbyla, D., Chapin, F.S., 2006. Methane bubbling from Siberian thaw lakes as a
585   positive feedback to climate warming. Nature 443, 71–75. https://doi.org/10.1038/nature05040

Wanninkhof, R., 1992. Relationship between wind speed and gas exchange over the ocean. J. Geophys. Res. 97, 7373–7382.
https://doi.org/10.1029/92JC00188

Whiticar, M.J., 1999. Carbon and hydrogen isotope systematics of bacterial formation and oxidation of methane. Chemical
Geology 161, 291–314. https://doi.org/10.1016/S0009-2541(99)00092-3

590 Wilson, J.F., Cobb, E.D., Kilpatrick, F.A., 1986. Fluorometric Procedures for Dye Tracing. Department of the Interior, U.S.
Geological Survey.

Yvon-Durocher, G., Allen, A.P., Bastviken, D., Conrad, R., Gudasz, C., St-Pierre, A., Thanh-Duc, N., del Giorgio, P.A., 2014.
Methane fluxes show consistent temperature dependence across microbial to ecosystem scales. Nature 507, 488–491.
https://doi.org/10.1038/nature13164

595 Zona, D., Gioli, B., Commane, R., Lindaas, J., Wofsy, S.C., Miller, C.E., Dinardo, S.J., Dengel, S., Sweeney, C., Karion, A.,
Chang, R.Y.-W., Henderson, J.M., Murphy, P.C., Goodrich, J.P., Moreaux, V., Liljedahl, A., Watts, J.D., Kimball,
J.S., Lipson, D.A., Oechel, W.C., 2016. Cold season emissions dominate the Arctic tundra methane budget.
Proceedings of the National Academy of Sciences 113, 40–45. https://doi.org/10.1073/pnas.1516017113